Role of slow dynamics in fast dynamics ultrasonic measurements

Role of slow dynamics in fast dynamics ultrasonic measurements

M.Scalerandi,[1,*)] C.Mechri,[2] M.Bentahar,[2] A. Di Bella,[1] A. S. Gliozzi,[1] and M. Tortello[1]

[1)] *Department of Applied Science and Technology (DISAT), Politecnico di Torino, Torino, 10129, Italy*

[2)] *Laboratoire d'Acoustique de l'Université du Mans (LAUM), Le Mans Université, Le Mans, 72085, France*

(Dated: 21 July 2020)

Nonlinear mesoscopic materials exhibit anomalous elastic nonlinearity in which fast and slow dynamics effects are mixed up. The former is an instantaneous nonlinear phenomenon due to the explicit strain dependence of velocity and damping. Slow dynamics is a non-equilibrium effect, governed by the dependence of the linear modulus and Q-factor on the dynamic strain level: when excited at constant strain, the sample properties vary in time (over minutes or more) until they reach a new equilibrium state. When excitation is removed, again slowly in time, the system recovers its original viscoelastic properties. The goal of this contribution is to show how slow dynamics might affect fast dynamics measurements and thus point out that care should be given to all time scales of the experiment, e.g. lag time between amplitude change and acquisition, duration of the acquisition and relaxation time between successive measurements.

[*)] marco.scalerandi@infm.polito.it

I. INTRODUCTION

Materials belonging to the class of mesoscopic nonlinear elastic materials[1], such as consolidated[2,3], unconsolidated[4] or damaged[5,6] granular media exhibit a peculiar nonlinear elastic behavior, in which effects at very different time scales can be observed (fast and slow dynamics)[7–11]. These materials are characterised by different microstructural features which respond to ultrasonic excitations with hysteresis in the stress-strain dependence[12].

Fast dynamics is generally associated to "instantaneous" variations of elastic modulus and damping coefficient[13–15] which are implicitly dependent on time and space, due to the explicit dependence of velocity and Q-factor on strain. Fast dynamics effects include generation of higher order harmonics[16,17], resonance frequency shift[18], break of the superposition principle[19], etc.

At the same time, each strain amplitude perturbing the material brings it to a new elastic state, different from the unperturbed one. However, this process is not instantaneous (it can take several minutes) and for this reason it is called slow dynamics. The effect, known since more than two decades[20–23], is due to the existence of different equilibrium states at different amplitudes of the strain perturbing the material. When a constant strain is applied, the material velocity and damping evolve slowly to an equilibrium value different from the unperturbed one. Once this new equilibrium is achieved (full conditioning) and maintained, the material properties do not change any more as long as a new strain level is not applied. The effect is reversible and once the strain is removed, slowly the system relaxes back to its original equilibrium (initial values of the material properties). This process is called relaxation. The new equilibrium state affects both linear material parameters[24,25] and nonlinear ones[26].

Effects of non-equilibrium (slow) and nonlinearity (fast) are mixed up when the material behavior is characterised, since the strain used to probe fast dynamics is responsible of conditioning as well. Furthermore, even though the time scales of fast and slow dynamics are much different, most of the effects of conditioning/relaxation take place in the first instants of time, thus are superimposed to fast dynamics effects, which are instantaneous. As a result, the same dynamic experiment conducted with different time intervals between successive acquisitions can in general give rise to different results. It has been shown by Tencate and Shankland[27] that in a resonance sweep the measured amplitude at each driving

frequency could be very different if a 30 seconds relaxation time is allowed between successive measurements. Later, Tencate and coworkers[28] have shown that the measured hysteresis in the nonlinear response of Berea can be very different if measurements are performed on a conditioned or not conditioned sample. The existence of conditioning effects on the two branches (at frequencies lower or higher than resonance) has also been well studied and presented as evidence of conditioning[29].

Slow dynamics could be considered a typical process that can be described by a time delay differential equation, taking into account the out of equilibrium dynamical process[30–32]. For a given applied excitation, an equilibrium state of the material is expected, with a certain modulus and damping different from those that describe the system when no excitation is applied. However, a time delay between the application of the conditioning perturbation and the reaching of equilibrium is present. Thus, two additional time scales are at play: the one of the duration of conditioning (related to the experimental protocol) and the equilibrium delay scale, which could often be of order of magnitudes different (e.g. from seconds to minutes). As shown in different systems, the interplay between the two time scales could lead to emerging nontrivial effects[32], which could affect the measurement itself.

While the existence of an entangling between slow and fast effects in the propagation of elastic waves in hysteretic media is normally accepted[34,35], the importance of specifying the time scales of the experimental protocol when performing dynamic ultrasonic measurements has not yet been correspondingly acknowledged and taken into account, except in a few cases (e.g.,[36,37]). From a more general point of view, considering the interplay between the time scale of the experimental protocol and the time-delay for reaching equilibrium could be important in view of fully establishing either an optimal experimental protocol or to take into account experimental observations, which are not intrinsic to the nonlinear properties of the medium. Our study could indeed be complementary to the analysis of the influence of other features related to the experimental set-up, which might contaminate the result of a measurement, such as imperfect boundary conditions[38,39] or uncontrolled clapping contacts[40].

Furthermore, in order to asses the role of the interplay between slow and fast dynamics (until now, in general, only qualitatively addressed) a quantification of the influence of the first on the latter, as a function of the experiment rate, is very desirable. It is however worth noticing here that quantitative results about the role of the experiment rate have been

presented only in the case of quasistatic (i.e low frequency) experiments so far, but these are not straightforwardly applicable to the dynamic case[12]. Finally, the quantitative relation between experiment rate and self conditioning, (i.e. the conditioning of the material induced by the propagating wave, which causes as a feedback a modification of the propagating wave itself) is one of the aims of the present paper.

II. MATERIALS AND METHODS

Experiments presented here were conducted using a waveform generator (Tektronix AFG 3022B) and working with ultrasonic signals defined as monochromatic waves of amplitude A_{inp} and frequency ν. After amplification through a linear amplifier (CIPRIAN Model US-TXP-3, 200 x), signals were transmitted to an ultrasonic transducer (with broadband response up to a few hundreds of kHz) acting as emitter. The transducer was glued to the sample using Phenyl Salicylate. A second (identical) transducer was used to detect the response of the material under test and was connected to a digital oscilloscope (Lecroy 324A) for data acquisition. Signals were recorded in a short time window once stationary conditions were reached (standing wave). Linearity of the acquisition system, including transducers and coupling, was verified. The frequency was chosen close to the first resonance mode ($\nu = 13.1$ kHz) and A_{inp} ranged from 10mV to 1.2V (before amplification).

The tested specimen was a concrete sample (B6) made in the shape of a cylinder (4 cm diameter and 16 cm length), drilled from a casting prepared with 340 kg of cement (CEM II A-L 42.5 R), 957 kg of sand (0-5 mm), 846 kg of gravel (5-15 mm) and 200 kg of water (w/c ratio ≈ 0.59). Samples were tested in a controlled environment. Temperature was fixed at $T = (26.0 \pm 0.2)\ ^o$C and relative humidity $R.H. = (39 \pm 2)\%$. Each measurement consisted in a given protocol of amplitudes as shown in Fig. 1. A relaxation time of about 16 hours was allowed between two successive measurements.

Nonlinearity was monitored using the Scaling Subtraction Method (SSM) indicator[13,19]. The indicator is defined as follows. First, the sample is excited at a low amplitude of excitation A_0 within the linear regime of the response of the sample. In our case $A_0 = 10mV$. A signal $u_0(t)$ is detected. Then, the sample is excited at larger amplitudes $A_i = m_i A_0 (i = 1...N)$ with different protocols for the choice of A_i, as shown in Fig.1. The signals $u_i(t)$ were detected and the *reference signals* $v_i(t) = A_i/A_0\ u_0(t)$ are constructed as the expected

linear response. From the difference between nonlinear and expected linear response, the *SSM signals* $w_i(t) = u_i(t) - v_i(t)$ are constructed. Any variation in velocity or attenuation as a function of amplitude results in a phase shift and amplitude variation of the signals $u_i(t)$ with respect to the expected linear response, thus in a variation (increase) of the SSM signal $w_i(t)$ as a function of amplitude. Finally, the *nonlinear SSM indicator*, defined as the maximum of the SSM signal, i.e. $\theta_i = \max(w_i(t))$, is plotted vs. the excitation level defined as $x_i = \max(u_i(t))$.

Different protocols of testing were implemented.

- Protocol-a represents a standard fast dynamics measurement: amplitude is increased from its linear value up to a maximum (upward branch) and then decreased back to its minimum value (downward branch). The measurement time was denoted with Δt_m (which was varied in our experiments from a few seconds to minutes) and represents the time lag between the instants in which the drive amplitude is changed and the acquisition is completed.

- Protocol-b represents a standard slow dynamics measurement: the amplitude is set at the minimum value and the linear signal is continuously detected. Afterward, the amplitude is switched at its conditioning level and kept constant while successive acquisitions are repeated. Finally, the amplitude is switched back to the linear value to monitor relaxation.

- Protocol-c represents a fast dynamics experiment in which the sample is kept always in a fully conditioned state: first, the sample is conditioned at high amplitude of excitation before measuring the linear signal (in our experiments A_c=1.25V, before amplification, Δt_c = 600 s and $\Delta t_m \approx 10s$). Afterwards, the input amplitude is increased and then decreased (recording an acquisition at each amplitude) to monitor the system response, always repeating the same conditioning excitation between successive acquisitions.

- Protocol-d represents a fast dynamics experiment in which the sample is kept in a fully conditioned state during the downward branch only.

The three fast dynamics protocols differ in the sense that in the protocol-a the nonlinear parameter monitors both nonlinearity and progressive conditioning/relaxation during up-

ward/downward branches, while in the protocol-c the nonlinear indicator is influenced only by nonlinearity. Protocol-d is introduced to avoid relaxation effects during the downward branch. Note that the acquisition time Δt_m is very short in protocols c and d to limit relaxation effects, while it is varied in protocol-a in order to modulate the relevance of progressive conditioning/relaxation.

III. FAST AND SLOW DYNAMICS

A. Experiments

Fast and slow dynamics experiments were conducted following protocols a and b reported in Fig. 1. Results are shown in Fig. 2. In subplot(a), we observe an increase of the nonlinear indicator when the excitation amplitude increases, typical of fast dynamics measurements (red circles). However, the measured nonlinearity is different in the downward branch (hysteresis) due to the conditioning induced by the probing wave.

Conditioning effects are discussed in subplot (b), where it is shown that the θ indicator does not immediately reach its asymptotic value once the conditioning amplitude is switched on (red circles). A significant conditioning time is observed (of the order of 10-15 minutes) during which nonlinearity varies up to 1 percent. In subplots (c) and (d), for sake of completeness, we also plot the evolution in time of the signal amplitude and phase (calculated fitting the recorded time signals with a sinusoidal function[41]). It is interesting to observe the decrease in amplitude and phase (increase in attenuation and softening) and their full recovery during relaxation.

B. Theory

Results shown in Fig. 2 suggest that velocity dependence on strain amplitude should contain two contributions: the first one is due to an instantaneous dependence on the actual strain, while the second one depends on the maximum strain amplitude and it is explicitly time dependent. In this section a theoretical framework will be outlined to describe the observed phenomenology.

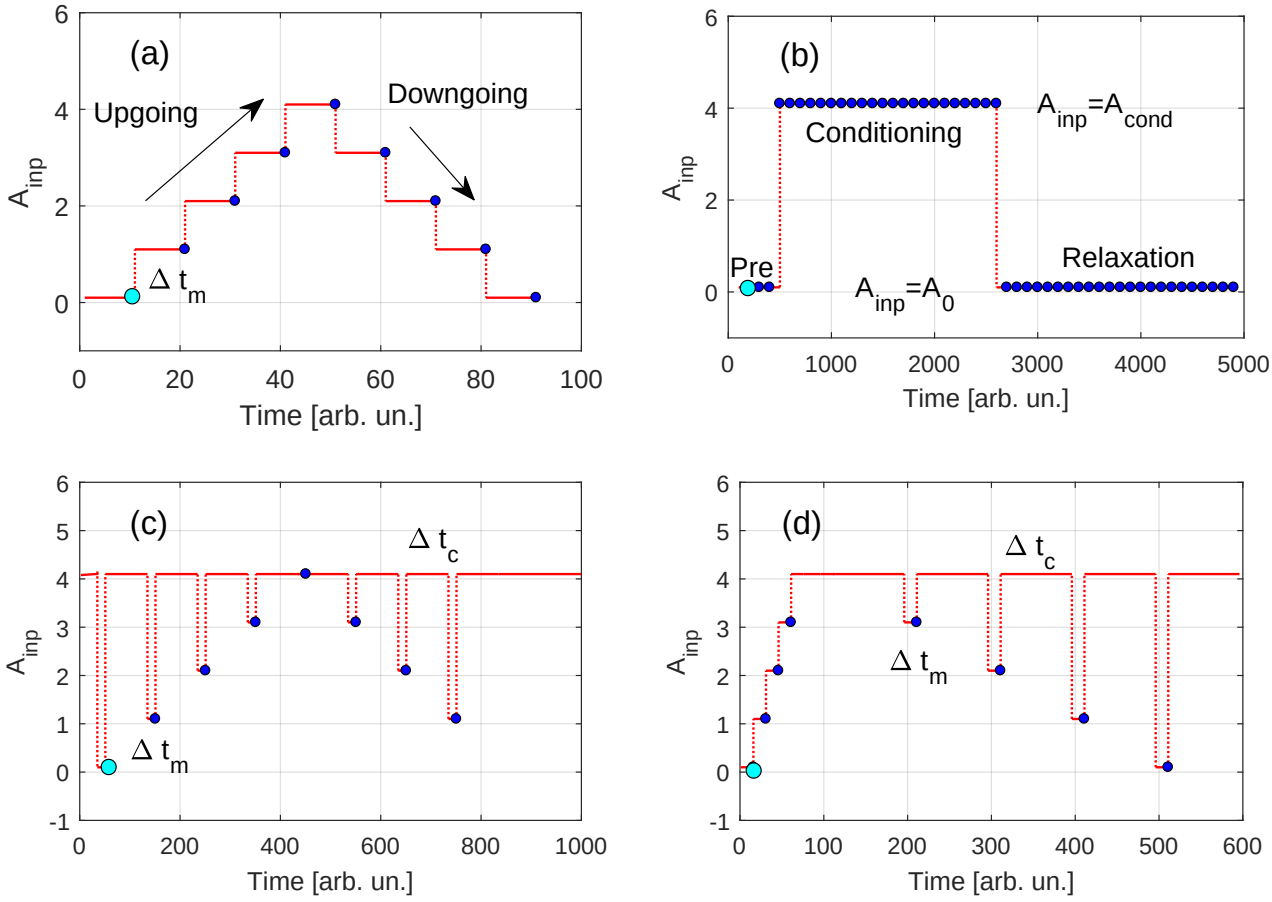

FIG. 1. Scheme of the experimental protocols chosen for the excitation amplitudes A_i. In all subplots, blue circles denote the time instants (and corresponding input amplitudes) at which measurements were performed, while cyan circles denote the time instant (and corresponding linear amplitude) at which the linear signal u_0 was detected. (a) Protocol for a standard fast dynamics measurement with progressive conditioning/relaxation effects (protocol-a); (b) Protocol for a standard slow dynamics measurement (protocol-b); (c) Protocol for a fast dynamics measurement on a sample in a fully conditioned state (protocol-c); (d) Protocol for a fast dynamics measurement on a sample without relaxation effects (protocol-d).

1. Conditioning and relaxation of an initially relaxed sample

Conditioning

Let us first consider the case in which we start with a fully relaxed sample. In particular, for each value of the strain, fast dynamics affects the velocity with an instantaneous term

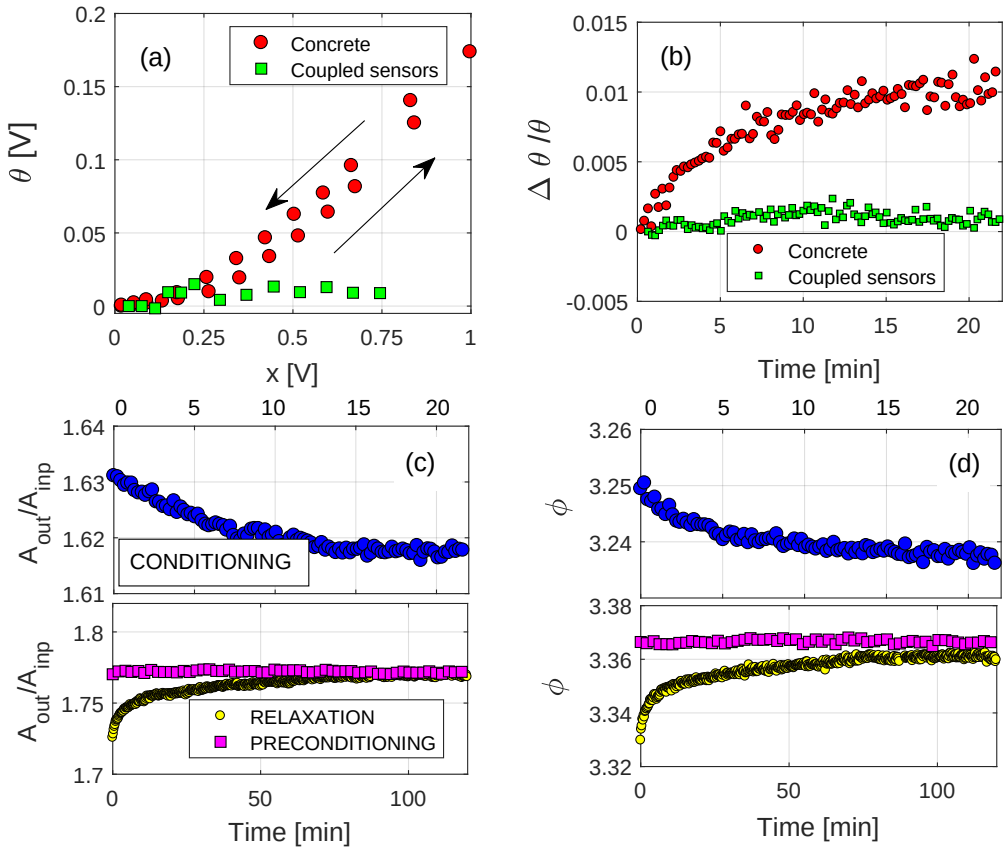

FIG. 2. Measurement of fast and slow dynamics. (a) Evolution of the nonlinear indicator θ for the upward/downward protocol-a shown in Fig. 1(a); (b) Variation of the nonlinear indicator θ vs. time during the conditioning phase of protocol-b shown in Fig. 1(b); (c) Evolution of signal amplitudes vs. time during conditioning and relaxation (protocol-b shown in Fig. 1(b)); (d) Evolution of signal phases vs. time during conditioning and relaxation (protocol-b shown in Fig. 1(b)). Results obtained measuring the direct transducer/transducer response (green squares) are shown to prove the linearity of the acquisition system in subplots (a) and (b).

δc_{NL} and conditioning is responsible of a non equilibrium contribution to velocity δc_{neq}. Assuming, for simplicity, that the two contributions are independent and defining c_L as the linear (low excitation amplitude) velocity, at a given amplitude of excitation A_i, during conditioning, the velocity c_i evolves with time as:

$$c_i = c_L - \delta c_{i,NL} - \delta c_{i,neq} f(t - t_c) \tag{1}$$

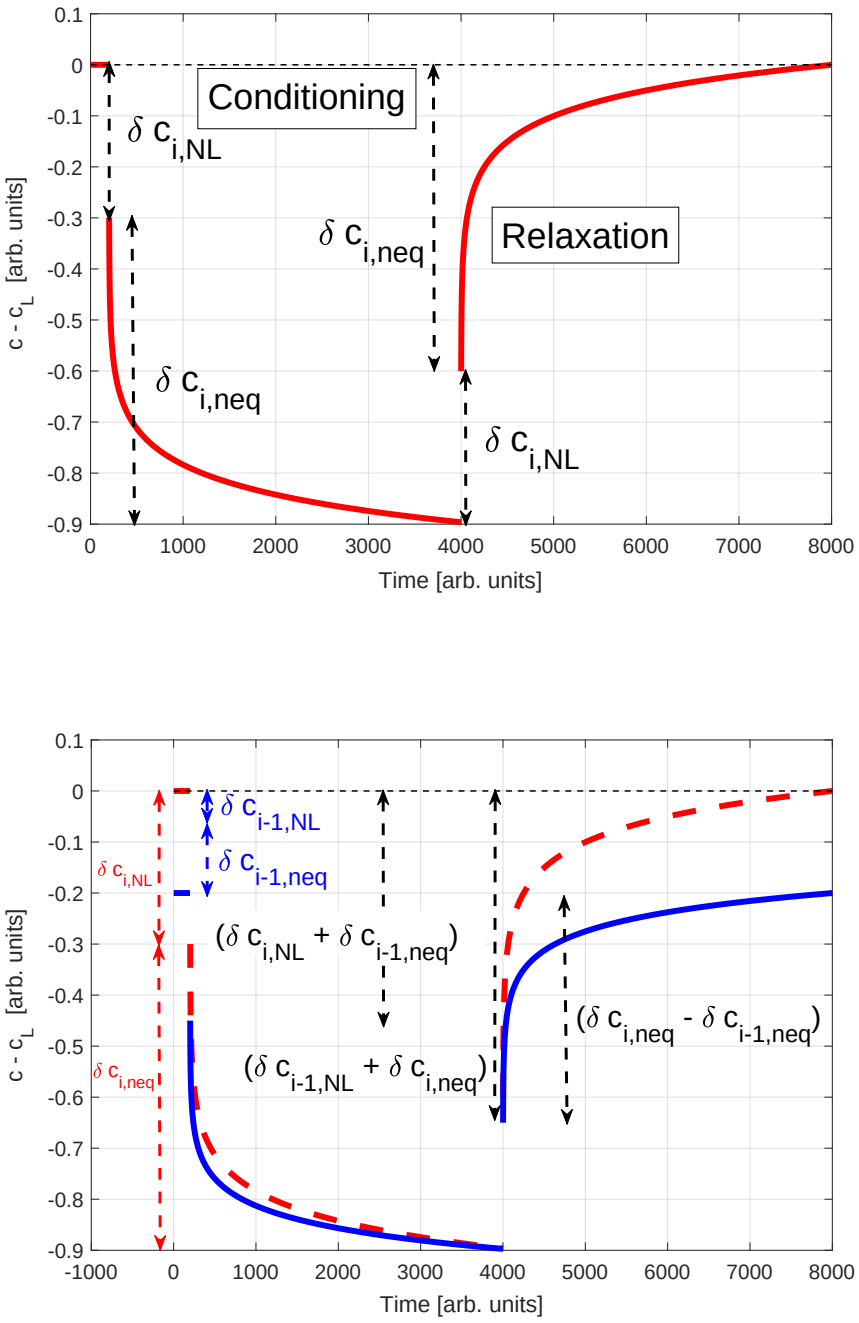

FIG. 3. Upper plot: Schematic predictions of the evolution of velocity when excitation amplitude is switched on (conditioning) and off (relaxation). Lower plot: Schematic predictions of the evolution of velocity when excitation amplitude is switched from A_{i-1} to A_i and back ($A_{i-1} < A_i$). The red dashed line corresponds to the red line in the upper plot and allows to appreciate differences when switching directly to excitation amplitude A_i starting from a fully relaxed sample.

where t_c is the instant at which conditioning starts and $f(t-t_c)$ is a monotonically increasing function satisfying the condition $f(0) = 0$ and $\lim_{t\to\infty} f(t - t_c) = 1$. The behavior is qualitatively illustrated in the upper plot of Fig. 3.

Time-delay description

Eq. 1 appears in the evolution equation of the propagating wave:

$$\frac{\partial^2 u}{\partial t^2} = \gamma \frac{\partial u}{\partial t} + c_i^2 \frac{\partial^2 u}{\partial x^2} \tag{2}$$

where u is the displacement, $\epsilon = \partial u/\partial x$ is the strain, γ an attenuation coefficient (containing also a delay term similar to that for c which will not be considered in the following discussion) and t and x are the time and space variables, respectively. Note that the attenuation contribution in Eq. 2 is a viscous term, which can be replaced with any other damping contribution model without affecting the discussion reported in the following.

Introducing the fast dynamic contribution δc_{NL} as in the classical nonlinear theory (first order), we can write

$$\frac{\partial^2 u}{\partial t^2} = \gamma \frac{\partial u}{\partial t} + \left(c_L - \beta \frac{\partial u}{\partial x} - \delta c_{i,neq} f(t - t_c) \right)^2 \frac{\partial^2 u}{\partial x^2} \tag{3}$$

where β is the first-order nonlinearity parameter (any other functional dependence for the fast dynamic nonlinear term could be considered without affecting the conclusions about the slow dynamics term). The wave propagation is essentially described by a nonlinear partial differential equation with a time-delay term (which introduces further nonlinear contributions).

In the following sections, we will investigate experimentally the role of the time-delay function. Experiments suggest that $f(t - t_c)$ should be described by a growing function with a time dependent growth rate, that can be approximated in its central part by a logarithmic function[34,42]. The temporal dependence of velocity/attenuation during conditioning allows to define one or more time scales[43], which represent a multiple delay behavior in the adjustment of the system to a new equilibrium.

Let us consider an elementary volume of the material which contains a certain number of potential defects N_0. Defects could have a modulus E_0 if not active or E_1 if active. Following the approach reported in ref.[44], the modulus of the elementary volume could be written as

$$E(t) = N_0\phi(t)E_1 + N_0\left(1-\phi(t)\right)E_0 = E(0) + \Delta E \tag{4}$$

where ϕ is the volume ratio of active defects and $E(0) = E_0N_0$. We recall that the wave velocity in a 1-D medium is $c = \sqrt{E/\rho}$. Therefore, by writing the Taylor expansion of $c(t)$ around $c_L = \sqrt{E(0)/\rho}$ we obtain:

$$\begin{aligned} c(t) - c_L &\propto \frac{1}{2}\Delta E = \frac{1}{2}\left(E(t) - N_0E_0\right) \\ c(t) - c_L &\propto \frac{1}{2}N_0(E_1 - E_0)\phi(t) \end{aligned} \tag{5}$$

During conditioning, the system evolves from a relaxed state to a new equilibrium. Thus ϕ should evolve from $\phi = 0$ to a new equilibrium value $\phi_{eq,i}$ which depends on the strain amplitude A_i at which the sample is excited. The number of defects out of equilibrium at time t is given as $\psi(t) = \phi_{eq,i} - \phi(t)$.

It follows:

$$c_i(t) - c_L \propto -\frac{1}{2}N_0(E_1 - E_0)\psi(t) + constant \tag{6}$$

where $E_1 < E_0$ (softening is always observed in experiments). Finally, using Eq. 1 we could calculate the evolution of the velocity variation during relaxation as

$$\Delta c = c_i(t) - c(t_c) = -\delta c_{i,neq} f(t - t_c) \tag{7}$$

From Eq. 6, we also obtain

$$\Delta c \propto \phi_{eq,i} - \psi(t) \tag{8}$$

If we consider a pure relaxation model, the concentration of defects out of equilibrium ψ decreases with a rate proportional to ψ:

$$\frac{d\psi}{dt} = -k\psi \tag{9}$$

and the classical exponential relaxation is found, which is not what has been experimentally observed in Fig. 2. To introduce multiple time scales in the relaxation process, we consider the decay rate not to be constant but dependent on a "triggering field" described by a spatially distributed quantity, which could describe e.g. fluids redistribution, formation

of sliding areas, dislocation nucleations, etc. This quantity evolves on a fractal domain (spatially), typical of the considered granular media. Therefore it evolves in time with a power law function (see e.g. the power law temporal behavior of fluids redistribution in fractal media[45,46] or the power law relaxation of elastic energy during damage processes in fractal domains[47]). Therefore:

$$k = k(t) = \alpha t^{\beta} \tag{10}$$

It follows that the solution for the temporal behavior of velocity during conditioning (and similar during relaxation and for the damping coefficient) is

$$\begin{aligned} \psi(t) &= \phi_{eq,i} e^{-(\frac{\alpha}{\beta+1})t^{\beta+1}} \\ \Delta c = c_i(t) - c(t_c) &= A(1 - e^{-(\frac{\alpha}{\beta+1})t^{\beta+1}}) \end{aligned} \tag{11}$$

where we assumed $t_c = 0$. The quantity $|\Delta c|$ is shown, on a semilog scale, in Fig. 4a for $\beta = -0.75, \alpha = 0.3$ and $A = 25$. Theoretical results are compared with experimental data. From the temporal evolution of phases and amplitudes measured on sample B03 (as shown in Fig. 2), the MoDaNE approach[41] allows to derive the temporal evolution of velocity. The velocity evolution $|\Delta c|$ during the conditioning time is shown in subplot (b). We observe an excellent agreement between the derived theoretical solution and experimental observations.

Of course the given equations still remain a simplified description to illustrate the behavior suggested by the experimental data of Fig. 2 and should be modified once a better knowledge of the specific system is available, but still they should maintain their main features.

Relaxation

As soon as the excitation is removed, velocity (and attenuation coefficient) slowly relax back to the linear value (measurements are assumed to be performed at a very low amplitude of excitation):

$$c_0 = c_L - \delta c_{i,neq} \left[1 - g\left(t - t_r\right)\right] \tag{12}$$

where t_r is the instant at which relaxation starts and $g(t - t_r)$ is again a monotonically increasing function satisfying the condition $g(0) = 0$ and $\lim_{t\to\infty} g(t - t_r) = 1$. The functions $f(t - t_c)$ and $g(t - t_r)$ could be different, even though experiments suggest the existence of

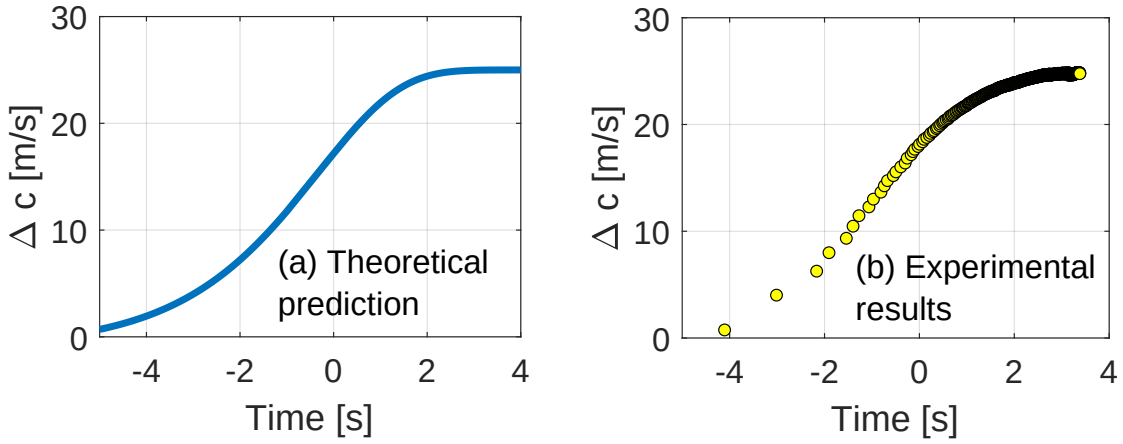

FIG. 4. (a) Representation of the analytical expression reported in Eq. 11. (b) Example of experimental results showing the temporal evolution of the velocity variation vs. time. Both plots are in a semilog scale to better appreciate the first instances of the evolution which deviate from a logaritmic behavior.

the same functional dependence for conditioning and relaxation. Similar considerations to those reported for the conditioning phase could be introduced here to describe the evolution during relaxation.

2. Conditioning and relaxation of an initially conditioned sample

The situation is more complicated when the sample is initially not completely relaxed, e.g. when the excitation amplitude is switched from one amplitude A_{i-1} to a larger amplitude A_i, as in the case of the upward branch of protocol (a) shown in Fig. 1. The equation describing the evolution of the velocity during conditioning at amplitude A_i becomes:

$$c_i = c_{i-1} - \chi_{i,i-1} - \Phi_{i,i-1} f(t - t_c) \tag{13}$$

where t_c is the instant at which the excitation amplitude is switched to the value A_i and $\chi_{i,i-1} = \delta c_{i,NL} - \delta c_{i-1,NL}$ and $\Phi_{i,i-1} = \delta c_{i,neq} - \delta c_{i-1,neq}$. The evolution is shown in the lower plot of Fig. 3. Similar considerations are valid to describe relaxation when the excitation

amplitude switches back to A_{i-1}:

$$c_{i-1} = c_i + \chi_{i,i-1} + \Phi_{i,i-1} g(t - t_r) \tag{14}$$

The lower plot of Fig. 3 allows to appreciate the interplay between non equilibrium states, their characteristic evolution time and the experimental protocol adopted. The different time-behavior between the blue and dashed red curves, e.g. during conditioning, is indeed a direct consequence of the delayed conditioning at amplitude A_i. As observed in other situations[30,32], a large time delay term in the equations, leading the system to equilibrium, implies a significant variation in the temporal evolution pattern, depending on the initial conditions of the sample, which could be the linear state, the equilibrium state corresponding to amplitude A_{i-1} (as in the plot) or a non-equilibrium state (not discussed here).

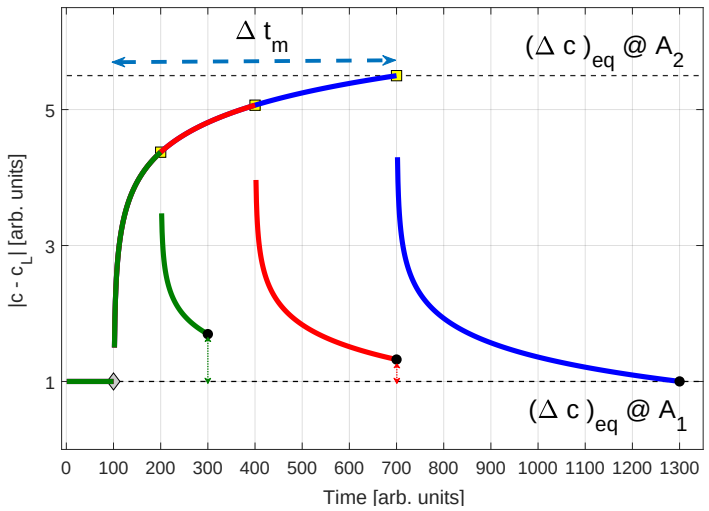

FIG. 5. Effects of the measurements duration Δt_m. Symbols denote times at which measurements are assumed to be performed in experiments. Different colours are referred to different measurement durations.

3. Expected behavior

Using the proposed dependence of velocity on nonlinear and non equilibrium terms, we have estimated the differences in measurement results depending on the chosen protocol and measurement duration Δt_m, when switching from amplitude A_1 to amplitude A_2 and back:

see Fig. 5. Lines of different colour display the velocity evolution for different measurement times and symbols denote the time instant at which the measurement is performed. As noticed, the longer Δt_m (blue line) the closer the measurement is taken to equilibrium and much higher is the variation of velocity from one amplitude to the next one (both upward and downward). When shorter measurement times are implemented (red and green curves) it can be noticed that, in the upward direction from A_1 to A_2 (from grey to yellow symbols measurements), smaller variations of velocity are expected since self conditioning did not have time to fully contribute. The same happens in the downward branch (from yellow to black symbols measurements) where full relaxation did not occur yet. As a consequence, the faster the measurement, the larger is the hysteresis observed, i.e. the larger is the difference between velocities at excitation amplitude A_1 before and after excitation at A_2 (from grey to black symbols, see also the small coloured arrows as a guide to the eye).

Theoretical expectations, even with a very simplified theory, agree with experimental results shown in the next Section. We also underline that the same considerations could be done for damping and/or other measurement protocols.

IV. EFFECTS OF SLOW DYNAMICS ON FAST DYNAMICS MEASUREMENTS

The theoretical discussion reported in the previous subsection suggests that measurement results strongly depend on the protocol and measurement time. In Fig. 6 we compare experimental results obtained from measurements following the protocols a, c and d (see Fig. 1). Results are therefore for fast dynamics experiments with amplitude increasing at its maximum and then decreasing back. Note that the three protocols differ in the amount of conditioning at maximum amplitude level introduced between subsequent measurements. In all cases Δt_m, i.e. the time lag between the amplitude variation and the acquisition, was set to 12s (very short). Results for the three protocols are shown in the left column of Fig. 6. In all cases, both upward and downward branches of the curves are well fitted by a power law function:

$$\theta = ax^b \tag{15}$$

The fitting function is reported as a solid line. The hysteresis between upward and downward

branches disappears when the experiments are performed on a fully conditioned sample (red), while it is larger when relaxation effects during the downward branch are inhibited (blue).

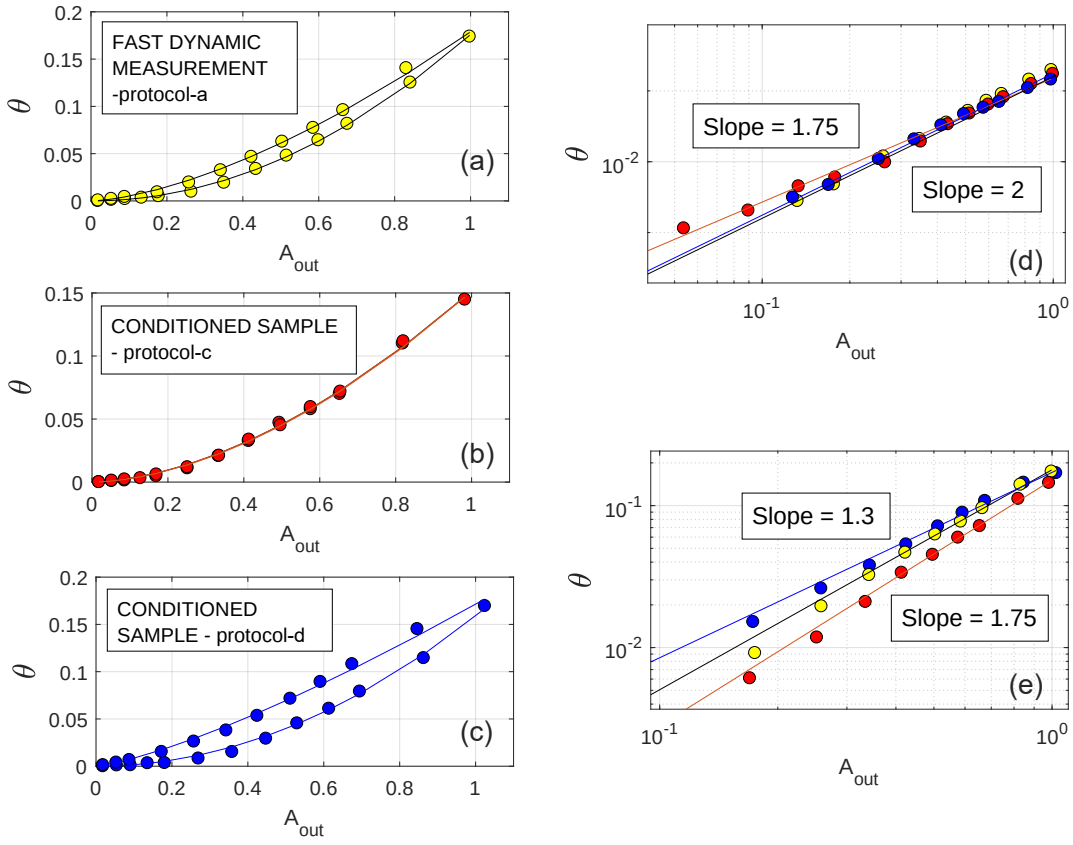

FIG. 6. Dependence of the nonlinear indicator on strain amplitude. (a): Upward and downward branches for protocol-a. Solid line is the fitting function reported in Eq. 15. (b): The same as in (a) but for protocol-c. (c): The same as in (a) but for protocol-d. (d) and (e): Comparison of the upward (d) and downward (e) branches in a log-log scale.

More interesting is the power law analysis performed in the subplots of the right column, where upward and downward curves for the three protocols are compared in a log-log scale. Starting from the upward branch, we notice that when the nonlinear indicators account for both conditioning and nonlinear features (protocols a and d), the slope of the curve (power law exponent b in Eq. 15) is equal to 2, as normally observed in the literature. On the contrary, the slope is slightly smaller when only nonlinear features are responsible of the increase of the nonlinear response (red symbols). In the downward branch case, relaxation effects cause a further change in slope, which approaches the value $b = 1.3$ for the case of

protocol-d. We recall that a slope $b = 1$ corresponds to noise effects only[48].

Focusing on protocol-a, the effects of the measurement time Δt_m on nonlinear fast dynamics measurements were analysed, as shown in Fig. 7. Results for increasing Δt_m are shown in the left column. As expected, longer acquisition times allow cumulative effects of self conditioning/relaxation in the upward/downward branches, resulting in a steeper increase of θ and reduction of the measured hysteretic effects. To quantify the analysis, Fig. 7 (d) reports the coefficient a (main panel) and exponent b (inset) of the power law fit of the upward branch data as a function of Δt_m. Whenever conditioning effects are present, in the upward branch the exponent remains $b \approx 2$ (also in the case of protocol-d reported for reference as a cyan symbol), while the exponent abruptly falls when the sample is permanently in a conditioned state (protocol-c), as shown by the pink symbol. The behavior of a vs. Δt_m is very well fitted by a logarithmic function (red solid line):

$$a = a_0 + a_1 log(\Delta t_m) \tag{16}$$

Panel (e) reports, as a function of Δt_m, the area of the hysteretic loop calculated by using the fitting functions of the upward and downward branches. As expected, the area increases with decreasing Δt_m, i.e. when reducing relaxation effects in the downward branch. The area is zero for a permanently conditioned sample (pink symbol, protocol-c), while it is maximum when relaxation is inhibited (cyan symbol, protocol-d). Again a logarithmic fit (red solid line) was performed, but the quality of the fitting is not as good as for the conditioning effect on a.

To further support the observations discussed above, additional tests were performed considering two other samples in the shape of prisms (3x3x15 cm^3):

- a mortar sample (TQ4) produced using Portland cement (CEM I 42.5N) with a water cement ratio w/c of 0.3 by mass;

- a civil engineering concrete sample (X2) produced with proportions of 2 cement volumes, 4 sand volumes and 6 gravel volumes every water volume (average gravel size is $(7 \pm 2)mm$ and sand particles size is predominantly around 2 mm). Sample X2 was damaged by quasi-static three point bending test performed at 25 percent of its rupture load.

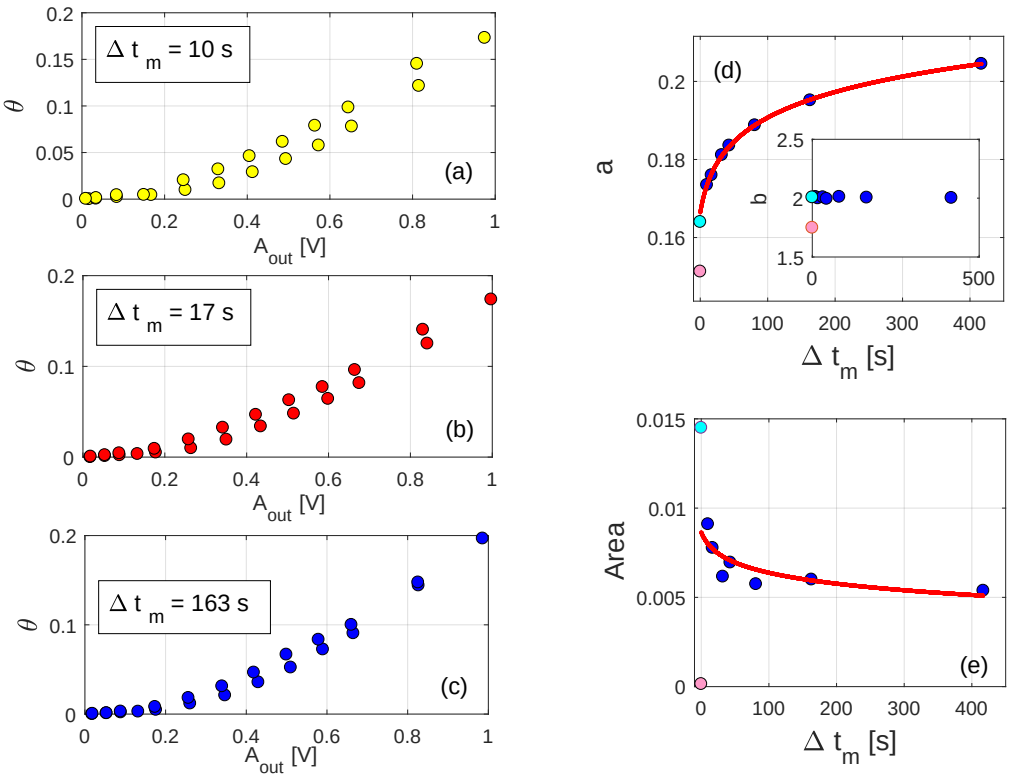

FIG. 7. Dependence of the nonlinear indicator on strain amplitude. (a), (b) and (c): Upward and downward branches for different duration of acquisition Δt_m in the case of protocol-a reported in Fig. 1(a). (d): Power law coefficient a and exponent b (in the inset) for the upward branch as a function of Δt_m. (e): Area of the hysteretic loop as a function of Δt_m. Cyan, pink and blue circles refer to a, b and area obtained from protocols d, c and a, respectively.

Results of the analysis are shown in Fig. 8. For the mortar sample TQ4 (left plot), protocol (a) was applied (both upward and downward branches for different measurement times Δt_m). Effects of increasing measurement time (red symbols) are significantly more visible than effects of slight random variations observed in repeated measurements at the same duration time (cyan and blue symbols). As it has already been observed in Fig.7, the longer the measurement time, the steeper the upward branch is and the smaller the area of the loop becomes.

Results for the upward branches of protocol (a) (different duration times) and (c) are compared for the X2 sample (right plot of Fig. 8). Repeatability of the measurements

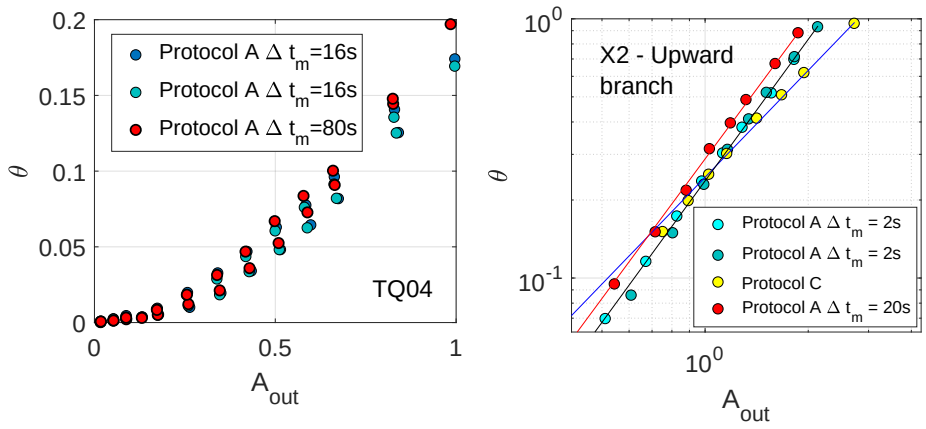

FIG. 8. Dependence of the nonlinear indicator on strain amplitude. Left plot: Sample TQ4. Upward and downward branches for different duration of acquisition Δt_m. Case of protocol (a) of Fig. 1. Right plot: Sample X2. Upward branch for different protocols and duration times in log-log scale. Solid lines are the power law fit.

(cyan and blue symbols) is excellent and the increase of the power law coefficient a with increasing Δt_m observed for the concrete and mortar samples is confirmed and reveals to be significant. Also, the reduction in slope (power law exponent b) when protocol (c) is applied, is evident, showing once again the important role that slow dynamics might play in fast dynamics experiments.

V. CONCLUSIONS

We have shown here that slow dynamics plays a significant role in fast dynamics experiments. Self conditioning, relaxation and the initial material equilibrium state are all contributing to the measured nonlinear response of hysteretic elastic samples, such as consolidated granular materials. Even though the time scale of full conditioning/relaxation is generally much longer than the time scale of a dynamic measurement, our results indicate that slow dynamics effects have to be considered when interpreting experimental data/measurements.

When considering standard fast dynamics experiments (upward branches of the curves) and the sample is initially fully relaxed, the effects of the acquisition duration (time scale) are small and probably negligible in practical applications. On the contrary, the acquisition

time has a huge effect on the determination of the amount of hysteresis (e.g. loop area). The knowledge of the initial equilibrium state (fully relaxed, fully conditioned or other combinations) is relevant for the determination of the correct power law dependence describing the behavior of nonlinearity vs. strain. The behavior observed experimentally results from the combination of an evolution equation with a time-delay term (in the form of Eq. 1), describing the transition of the sample to a new equilibrium state. When the experimental time scale does not match the characteristic time-delay constant, the observed/measured amount of hysteresis, which is strongly dependent on the initial state at each measurement, could be strongly affected.

Considering all experimental time scales (e.g. relaxation time between successive experiments and duration of the acquisition) is thus of great relevance for a correct estimation of the material nonlinear properties. In principle, long acquisitions (i.e. measurements taken always in equilibrium state) are less sensitive to transient/uncontrollable effects. However, these protocols are often difficult to realise in practice being extremely time consuming and more easily affected by environmental variations in temperature and humidity on such a long time scale.

REFERENCES

[1]R.A.Guyer, P.A.Johnson, Nonlinear Mesoscopic Elasticity, Wiley-VCH, 2009.

[2]P.Antonaci, C.L.E.Bruno, P.G.Bocca, M.Scalerandi, A.S.Gliozzi, Cem.Concr.Res. 40, 2010, 340-346.

[3]R.A.Guyer, J.Tencate, P.A.Johnson, Phys.Rev.Lett. 82, 1999, 3280-3283.

[4]V. Y. Zaitsev, V. E. Gusev, V. Tournat, and P. Richard, Phys. Rev. Lett. 112, 2014, 108302.

[5]I.Solodov, G.Busse, Appl. Phys. Lett. 102, 2013, 061905.

[6]M.Scalerandi, S.Idjimarene, M.Bentahar et al., Communications in Nonlinear Science and Numerical Simualtions 22, 2015, 334-347.

[7]M.Scalerandi, A.S.Gliozzi, C.L.E.Bruno, P.Antonaci, Physical Review B 81, 2010, 104114.

[8]P.Shokouhi, J.Riviére, R.A. Guyer, and P.A. Johnson, Appl.Phys.Lett. 111, 2017, 251604.

[9]M.Remillieux, R.A. Guyer , C. Payan, T.J. Ulrich, Phys.Rev.Lett. 116, 2016, 115501.

[10]M.Lott, M.C.Remillieux, V.Garnier, P.-Y. Le Bas, T. J. Ulrich, and C. Payan, Phys Rev.

Mat. 1, 2017, 023603.

[11]J.A.Bittner, J.S.Popovics, Appl.Phys.Lett. 114, 2019, 021901.

[12]K.E.Claytor, J. R. Koby, J. A. TenCate, Geoph. Res.Lett. 36, 2009, L06304.

[13]M.Scalerandi, M.Bentahar, C.Mechri, Construction and Building Materials 161, 2018, 208-220.

[14]C.Trarieux, S. Callé, H. Moreschi, G. Renaud, and M. Defontaine, Appl. Phys. Lett. 105, 2014, 264103.

[15]R.K.Gazizov, N.H.Ibragimov, O.V.Rudenko, Communications in Nonlinear Science and Numerical Simulations 19, 2014, 337-344.

[16]G.Kim, J.-Y.Kim,K. E.Kurtis, L. J.Jacobs, Cem.Concr.Res. 92, 2017, 16.

[17]J.-J. Sinou, Communications in Nonlinear Science and Numerical Simulations 13, 2008, 2024-2040.

[18]M.Bentahar, H. El Aqra, R. El Guerjouma, M. Griffa, M. Scalerandi, Phys. Rev.B 73, 2006, 014116.

[19]M.Scalerandi, A. S. Gliozzi, C. L. E. Bruno, D. Masera and P. Bocca, Appl.Phys.Lett. 92, 2008, 101912.

[20]J.A.TenCate, E.Smith, R.A.Guyer, Phys. Rev. Lett. 5, 2000, 1020-1023

[21]R.A.Guyer, K.R.McCall, K. Van den Abeele, Geoph.Res.Lett. 25, 1998, 1585-1588.

[22]A.Astorga, P. Guéguen, T. Kashima, Bull.Seism.Soc.Am. 108, 2018, 1185-1198.

[23]M.Nobili, M.Scalerandi, Physical Review B 69, 2004, 104105.

[24]J.Rivière, G.Renaud, R.A.Guyer and P.A.Johnson, J.Appl.Phys. 114, 2013, 054905.

[25]M.Scalerandi, A.S.Gliozzi, M.Ait Ouarabi, F.Boubenider, Appl.Phys.Lett. 108, 2016, 214103.

[26]C.Mechri, M.Scalerandi, M.Bentahar, Communications in Nonlinear Science and Numerical Simulation 45, 2017, 117-128.

[27]J.A. TenCate, T.J.Shankland, Geoph.Res.Lett. 23, 1996, 3019-3022.

[28]J.A. TenCate, D. Pasqualini, S. Habib, K. Heitmann, D. Higdon, P.A. Johnson, Phys.Rev.Lett. 93, 2004, 065501.

[29]P.A.Johnson, B.Zinszner, P.N.J.Rasolofosaon, J.Geoph.Res. 101, 1996, 11553-11564.

[30]J.Cermak, T.Kisela, Communications in Nonlinear Science and Numerical Simulations 79, 2019, 104888.

[31]Q.Yao, L.Wang, Y.Wang, Communications in Nonlinear Science and Numerical Simula-

tions 78, 2019, 104865.

[32]D.Bratsum, I.Krasnyakov, A.Zyuzgin, Communications in Nonlinear Science and Numerical Simulations 47, 2017, 109-126

[33]X.Wang, L.Wang, J.Wu, Communications in Nonlinear Science and Numerical Simulations 70, 2019, 80-88

[34]P.A. Johnson, A. Sutin, J.Acoust.Soc.Am. 117, 2005, 124-130.

[35]M.Lott, C. Payan, V. Garnier, Q.A. Vu, J.N. Eiras, M.C. Remillieux, P.-Y. Le Bas, and T. J. Ulrich, Appl.Phys.Lett. 14, 2016, 141907.

[36]J.A. TenCate, Pure and Applied Geoph. 168, 2011, 2211-2219.

[37]M. Scalerandi, A.S. Gliozzi, C.L.E. Bruno, P. Antonaci, Journal of the Acoustical Society of America 131, 2012, 4304-4315

[38]T.Roncen, J.P.Lambelim, J.-J.Sinou, Communications in Nonlinear Science and Numerical Simulations 74, 2019, 14-29.

[39]H.Farokhi, M.R.Paidoussis, A.K.Misra, Communications in Nonlinear Science and Numerical Simulations 65, 2018, 272-298.

[40]I.Kirrou, M.Belhag, Communications in Nonlinear Science and Numerical Simulations 18, 2013, 2916-2925.

[41]C. Mechri, M. Scalerandi, M. Bentahar, Phys.Rev.Appl. 11, 2019, 054050

[42]M.Scalerandi, C.Mechri, M.Bentahar, A.Di Bella, A.S.Gliozzi, M.Tortello, Phys.Rev.Appl. 12, 2019, 044002

[43]P.Shokouhi, J.Riviere, R.A.Guyer, P.A.Johnson, Applied Physics Letters 111, 2017, 251604.

[44]L.Ostrovsky et al., J.Geoph.Res. Solid Earth 124, 2019, 5003

[45]M.Filipovitch et al., Water Resources Research 52, 2016, 5167

[46]S.Zhang, Y.Zhang, B.Wang, Int. J. Heat and Mass Transfer 113, 2017, 1093.

[47]N.Pugno, F.Bosia, A.S.Gliozzi et al., Phys.Rev.E 78, 2008, 046103.

[48]M. Bentahar, R. El Guerjouma, S. Idijmarene, M. Scalerandi, J.Appl.Phys. 113, 2013, 043516.